

ISSN: 1674-0815

cjhmonline.com

DoI-10.564220/1674-0815

Chinese Journal of Health  
Management

Chinese Medical Association



## Formulation and In Vitro Evaluation of an Oral Osmotic Drug Delivery System for Valacyclovir

Sachinendra Ishwar Singh<sup>1</sup>, Vikram Singh Sisodiya<sup>2</sup>, Ajay Pal Singh<sup>3</sup>, Dipti R. Kute<sup>4</sup>, Rohini P. Zambade<sup>5</sup>, Sanket Gabhale<sup>6</sup>, Kris Jain<sup>7</sup>

<sup>1,2,3,7</sup>Anjali College of Pharmacy & Science, NH-2, Agra Firozabad Road, Etmadpur, Agra, Uttar Pradesh, 283202, India <sup>4,5</sup> Sharad Chandra Pawar college of Pharmacy, otur, Pune

<sup>6</sup> University of Mumbai

Corresponding Author Email id: [sachinendrasingh00729@gmail.com](mailto:sachinendrasingh00729@gmail.com), [krisjainsafeshop2lakh@gmail.com](mailto:krisjainsafeshop2lakh@gmail.com)

### Article Information

Received: 15-10-2025

Revised: 04-11-2025

Accepted: 24-11-2025

Published: 26-12-2025

### Keywords

*Valacyclovir, Controlled porosity osmotic pump, Sustained release, Cellulose acetate, Antiviral therapy, Patient compliance*

### ABSTRACT:

Valacyclovir, an antiviral prodrug of acyclovir, is commonly prescribed for the treatment of herpes virus infections. Despite its clinical benefits, its short half-life and limited oral bioavailability necessitate frequent dosing, which can reduce patient adherence. To address these drawbacks, the ongoing study focused on formulating-controlled porosity osmotic pump (CPOP) tablets of valacyclovir to ensure prolonged and regulated drug delivery. Core tablets were formulated via wet granulation and subsequently coated with a semipermeable membrane comprising cellulose acetate and pore-forming agents, enabling controlled water ingress and sustained drug release through osmotic pressure modulation. Pre-formulation studies, including solubility assessment of drug–excipient interactions evaluation, were executed to aid formulation design. The tablets were tested for hardness, breakability, thickness, and even distribution of the drug. In vitro release experiments conducted in 0.1 N HCl and phosphate buffer (pH 7.4) indicated a sustained drug release profile, a pH-independent drug release trend consistent with osmotic-controlled delivery. Morphological analysis by SEM

### ©2025 The authors

This is an Open Access article

distributed under the terms of the Creative Commons Attribution (CC BY NC), which permits unrestricted use, distribution, and reproduction in any medium, as long as the original authors and source are cited. No permission is required from the authors or the publishers. (<https://creativecommons.org/licenses/by-nc/4.0/>)

demonstrates uniform pore formation on the membrane surface after dissolution, while FTIR and DSC evaluations demonstrated the absence of significant interactions between valacyclovir and excipients. Accelerated stability testing revealed no notable changes in drug content or release profile. The optimised CPOP tablets successfully provided extended release of valacyclovir, suggesting improved bioavailability and reduced dosing frequency. This formulation strategy presents a promising approach to enhance the therapeutic performance of valacyclovir and improve patient compliance in antiviral therapy.

**INTRODUCTION:**

Valacyclovir is an ester prodrug derived from acyclovir and is commonly administered for treating herpes simplex, herpes zoster, and varicella, which are significant viral infections. Despite its clinical significance, its use is restricted due to an abbreviated half-life and inconsistent oral absorption, necessitating frequent dosing to achieve and sustain therapeutic concentrations in plasma. These limitations often reduce patient compliance and have the potential to yield non-uniform therapeutic results. An oral osmotic advanced delivery platforms present a feasible approach for resolving these problems. Osmotic systems use the principle of osmosis to regulate drug release, providing a constant and predictable release profile that is largely independent of gastrointestinal conditions such as pH or motility. By incorporating Valacyclovir into an osmotic delivery platform, the drug can be released gradually over time, ensuring more stable plasma concentrations, reduced dosing frequency, and improved patient adherence. This approach enhances the clinical effectiveness of Valacyclovir while minimising the drawbacks of conventional oral formulations, making it a rational choice for long-term antiviral therapy.<sup>1</sup> For effective treatment, a good drug delivery system should provide the required amount of medicine for a suitable time span. Since many drugs show prolonged retention in the body only for a short duration, repeated dosing is often needed to maintain the desired blood levels. To address this issue, controlled and long-acting release formulations (Figure 1.1) are being widely scrutinised in the pharmaceutical field.<sup>ii</sup>

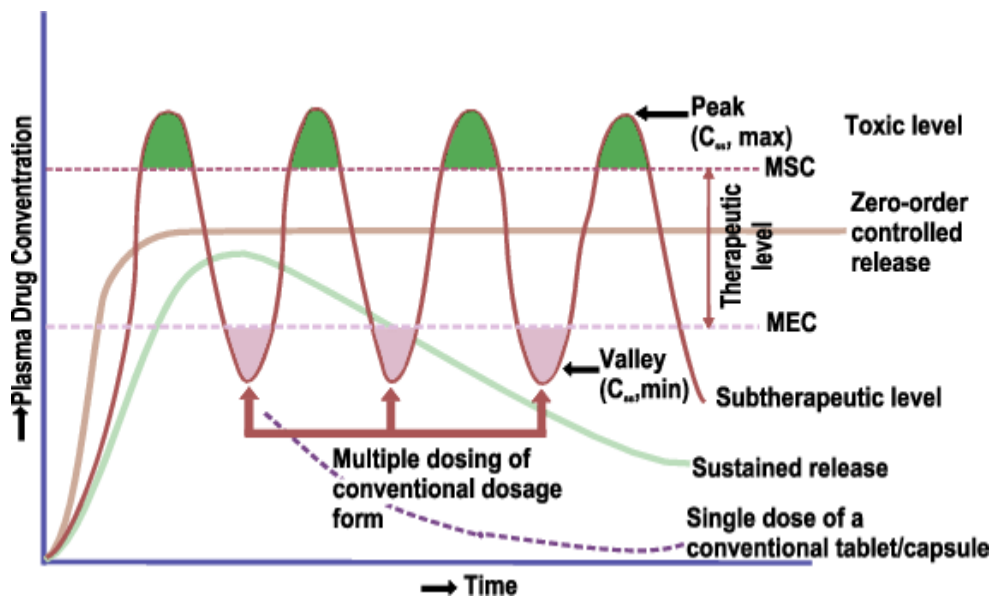


Figure 1: Diagrammatic representation of Time-dependent plasma concentration profiles (C-t curve) for conventional, sustained release and controlled release preparations.

Orally controlled drug delivery results in drug liberation across the GI tract via Diffusion, dissolution, or concurrent mechanisms. The physical form and molecular profile of the drug, such as crystal form, solubility, partition coefficient, and intrinsic dissolution rate, significantly influence the formulation’s performance and optimisation. Unlike conventional dosage forms, targeted oral delivery systems are engineered to enhance therapeutic outcomes by improving the drug’s pharmacokinetic profile, while also increasing patient convenience and adherence to treatment.<sup>iii-v</sup>

**Types of Oral Timed-Release Drug Delivery System**

Emerging trends in pharmaceutical sciences research have driven the progress of novel oral controlled delivery of drug strategies. The primary aim of such systems is to transform an active drug molecule, which may have unfavourable physicochemical or physiological properties, into a formulation that provides optimal therapeutic

©2025 The authors

This is an Open Access article

distributed under the terms of the Creative Commons Attribution (CC BY NC), which permits unrestricted use, distribution, and reproduction in any medium, as long as the original authors and source are cited. No permission is required from the authors or the publishers. (<https://creativecommons.org/licenses/by-nc/4.0/>)

performance. These systems are designed to maintain sustained therapeutic drug levels while offering additional advantages, such as:<sup>vi-viii</sup>

- Improved bioavailability
- Minimised inter-patient variability
- Flexible and tailored release profiles
- Prolonged time between doses
- Promoted adherence to treatment
- Lower incidence of side effects

**Osmotic drug delivery systems (ODDS):** Osmotic pump-based release formulations represent one of the most advanced approaches in oral controlled-release technology. The concept was first introduced by Australian scientists Rose and Nelson in 1955, who designed a three-chamber implantable osmotic pump. Later, in the 1970s, Alza Corporation simplified this design, which improves its practical for pharmaceutical practical applications (Vyas et al., 2001). The original Rose–Nelson pump was subsequently refined into the original Higuchi–Leeper osmotic delivery device. Later refined by Higuchi and Theeuwes, contributing a streamlined version of the system. The launch of the oral therapeutic delivery facilitated by an EOP (elementary osmotic pump) drug delivery platform in 1975 was a significant milestone, establishing the foundation for modern osmotic delivery systems

Osmotic drug delivery platforms afford several benefits over conventional and alternative regulated-release formulations. These include:

- 1 Provides a controlled and nearly zero-order drug release over an extended duration.
- 2 Drug release remains largely unaffected by variations in pH, food intake, or gastrointestinal motility.
- 3 Maintains steady plasma concentrations, thereby improving overall bioavailability.
- 4 Prolongs therapeutic action, thereby minimising the frequency of administration.

#### **Limitations associated with osmotic drug delivery systems<sup>xi-x</sup>**

While Osmotic configurations are capable of providing several advantages, they also present certain challenges and limitations that restrict their universal application. These include:

- 1 High manufacturing cost due to specialised design and technology requirements.
- 2 Possibility of dose dumping if the system is physically damaged.
- 3 Limited applicability for drugs having very short half-lives, since achieving therapeutic levels would require high doses.
- 4 Limited use for drugs with poor water solubility, as osmotic systems depend on water influx.

#### **Principle of Osmosis:**

Osmotically driven drug delivery device function guided by the concept of osmosis, wherein a solvent—Water tends to flow across a semipermeable membrane from a solution with lower solute content toward a hypertonic region until equilibrium is reached. In these systems, gastrointestinal fluids act as the external solvent and penetrate the rate-regulating coating covering the dosage form. This inflow of fluid dissolves the drug or creates hydrostatic pressure inside the core, driving the drug solution outward via a precision-drilled orifice at a regulated and predictable rate. Consequently, osmotic systems provide prolonged and consistent drug release.<sup>xi-xiii</sup>

©2025 The authors

This is an Open Access article

distributed under the terms of the Creative Commons Attribution (CC BY NC), which permits unrestricted use, distribution, and reproduction in any medium, as long as the original authors and source are cited. No permission is required from the authors or the publishers. (<https://creativecommons.org/licenses/by-nc/4.0/>)

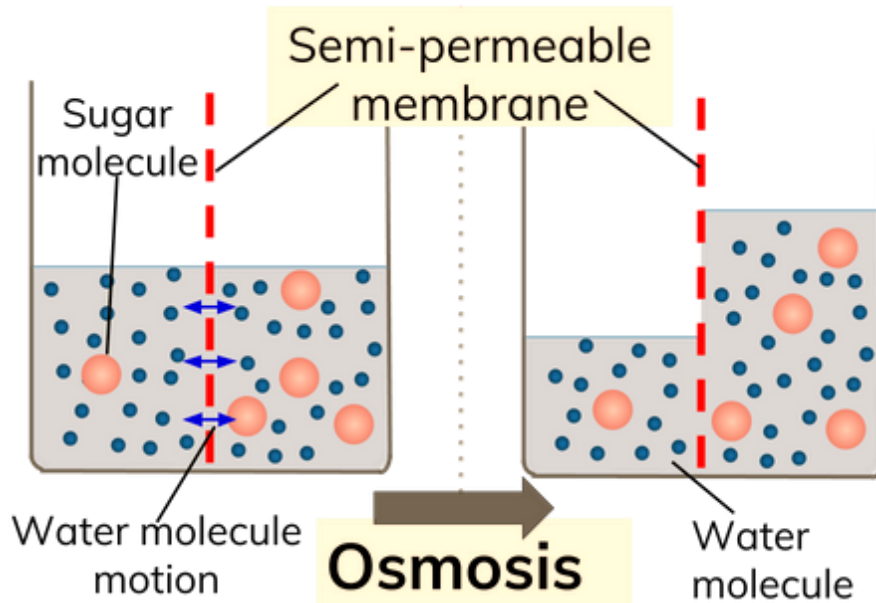


Figure 2: Schematic representation based on osmotic flow and the establishment of osmotic equilibrium

### Hierarchical Organisation of Osmotic-mediated drug delivery Mechanisms

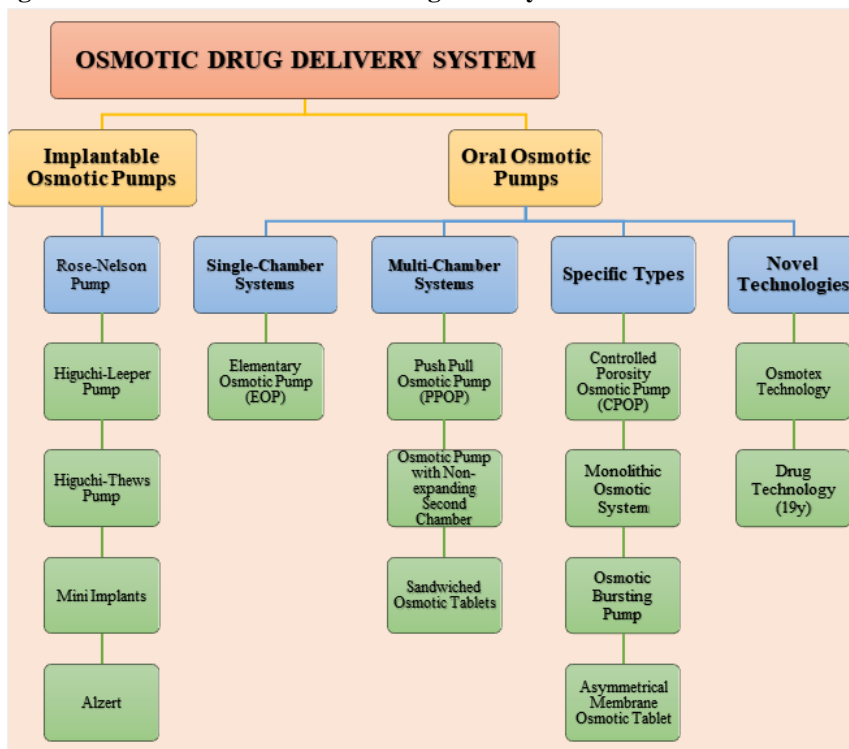


Figure 3: Advanced Osmotic-mediated controlled release systems are categorised as implantable devices, single- or multi-chamber pumps, and modified oral osmotic systems<sup>xiv</sup>

### Pioneers of modern osmotic pumps:

#### Rose-Nelson Pump:

In 1955, Australian physiologists introduced osmotic drug delivery with the first osmotic pump for controlled administration in animals. The system included a drug reservoir, salt chamber with elastic diaphragm, and delivery orifice. Water influx through a semipermeable membrane generated pressure to drive drug release at a

©2025 The authors

This is an Open Access article

distributed under the terms of the Creative Commons Attribution (CC BY NC), which permits unrestricted use, distribution, and reproduction in any medium, as long as the original authors and source are cited. No permission is required from the authors or the publishers. (<https://creativecommons.org/licenses/by-nc/4.0/>)

constant rate, independent of pH or motility, forming the basis of modern oral osmotic delivery platforms.<sup>xv</sup>

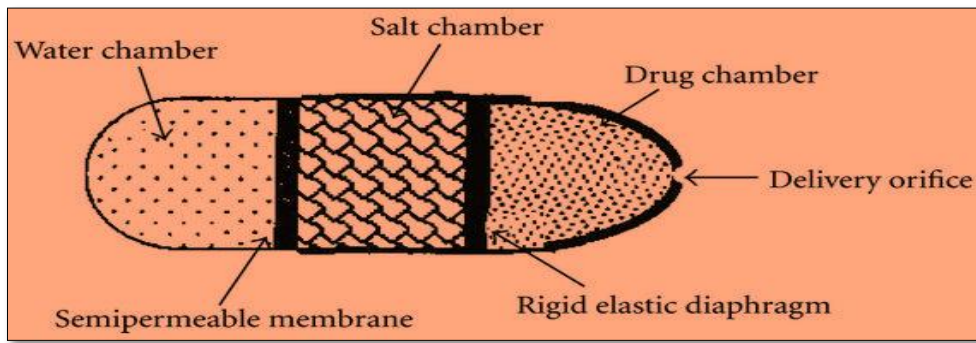


Figure 4: Underlying configuration of Rose–Nelson controlled-release pump

### Higuchi Leeper Pump:

The Higuchi–Leeper engineered osmotic controlled-release pump, an evolution relating to the Rose–Nelson system, has found extensive use in veterinary applications for controlled delivery of therapeutic agents, including antibiotics and growth hormones. Its design incorporates a rigid casing, a semipermeable membrane, and a waxy barrier dividing the drug and osmotic chambers. A key innovation of this design was the introduction of pulsatile drug release, achieved by generating critical osmotic pressure to open the delivery orifice, followed by closure as the pressure dropped. This cyclical mechanism enabled burst release of the drug at controlled intervals, preventing premature leakage and establishing the pump as a prototype for modern pulsatile osmotic delivery systems.<sup>xvi</sup>

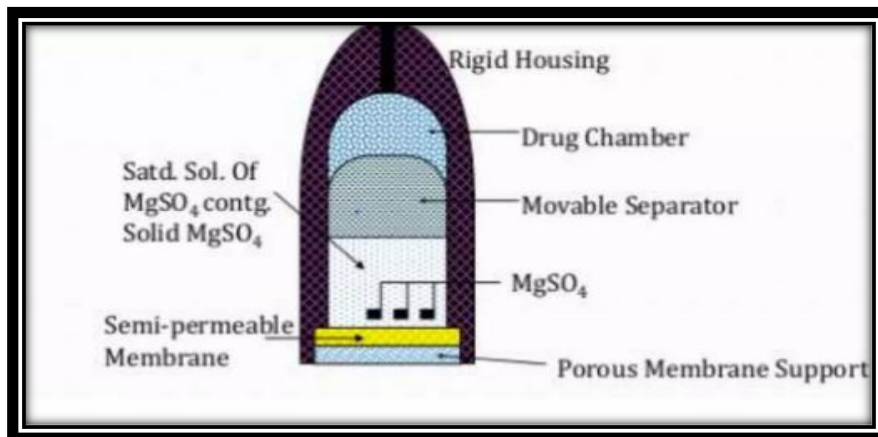


Figure 5: Conceptual illustration of the Higuchi–Leeper pump

### Higuchi -Theeuwes Pump

In the early 1970s, Higuchi and Theeuwes introduced a streamlined Rose–Nelson pump, similar to the Higuchi–Leeper design, incorporating a push compartment for sustained release. Water entry through the semipermeable membrane generated osmotic pressure, eliminating the need for a rigid enclosure. The durable membrane acted as the outer shell, regulating drug release based on salt type and membrane permeability. Most pumps used granular salt in a carrier to maintain osmotic pressure, ensuring consistent and prolonged drug delivery.<sup>xvii-xviii</sup>

©2025 The authors

This is an Open Access article

distributed under the terms of the Creative Commons Attribution (CC BY NC), which permits unrestricted use, distribution, and reproduction in any medium, as long as the original authors and source are cited. No permission is required from the authors or the publishers. (<https://creativecommons.org/licenses/by-nc/4.0/>)

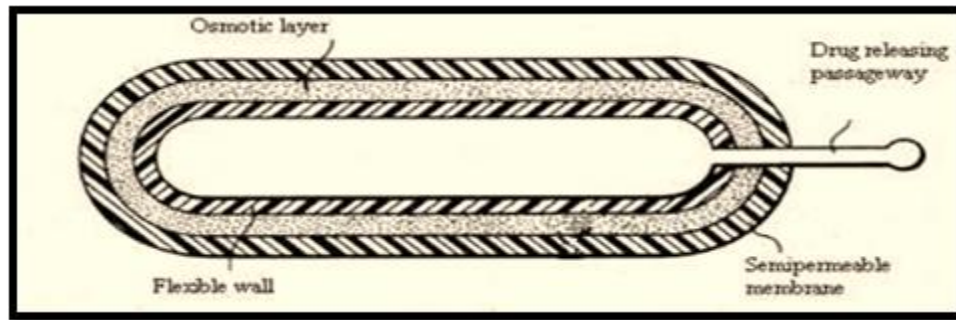


Figure 6: Mechanistic diagram of the Higuchi–Theeuwes pump

**Classification of Oral Osmotic Pumps:**

**1. Single-chamber osmotic pumps:**

**Elementary osmotic pump (EOP):**

Theeuwes subsequently pioneered the basic osmotic pump (EOP), a simplified and robust system for controlled drug delivery. The device comprises a central tablet comprising the active pharmaceutical ingredient along with suitable water-attracting agents, enclosed within a permselective membrane, typically made of cellulose acetate. A compact orifice is an opening formed in the membrane to allow controlled drug release. Being subjected to the environment leads to water influx toward the inner core, driven by osmotic forces and pressure differences, producing a fully concentrated drug solution. Because the membrane is inelastic, the incoming water generates hydrostatic pressure that initiates the saturated solution to release via the outlet, ensuring uniform and sustained drug administration.<sup>xix-xx</sup>

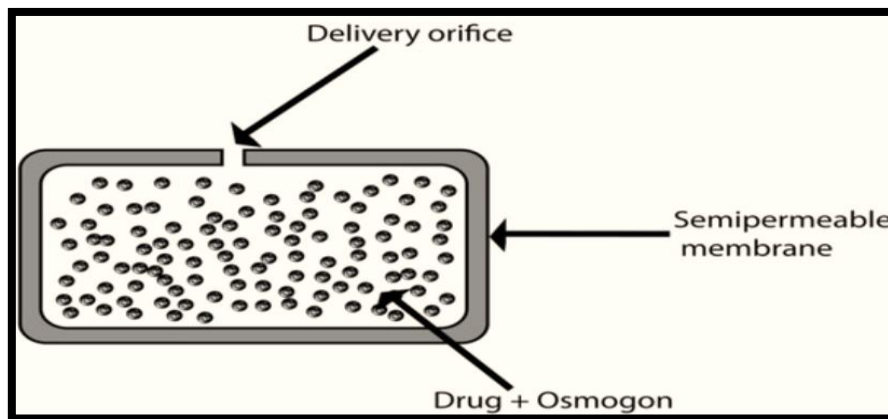


Figure 7: Working principle of the Elementary Osmotic Pump

**2. Multi-chamber osmotic pump:**

**Push-pull osmotic pump:**

The push–pull osmotic pump (PPOP) acts as an advanced bilayer system that enables controlled administration of therapeutic agents exhibiting low and high hydrophilicity. It comprises a drug layer that includes the active pharmaceutical ingredient along with osmotic agents and excipients, together with a push layer composed of swellable polymers and osmotic agents. A membrane allowing selective passage coats the bilayer core, with a tiny delivery orifice positioned on the drug-layer side. Upon exposure to an aqueous medium, the drug layer forms a solution or suspension, while the push layer swells and generates pressure, ensuring a constant and controlled expulsion of the drug via the exit orifice.<sup>xxi-xxii</sup>

©2025 The authors

This is an Open Access article

distributed under the terms of the Creative Commons Attribution (CC BY NC), which permits unrestricted use, distribution, and reproduction in any medium, as long as the original authors and source are cited. No permission is required from the authors or the publishers. (<https://creativecommons.org/licenses/by-nc/4.0/>)

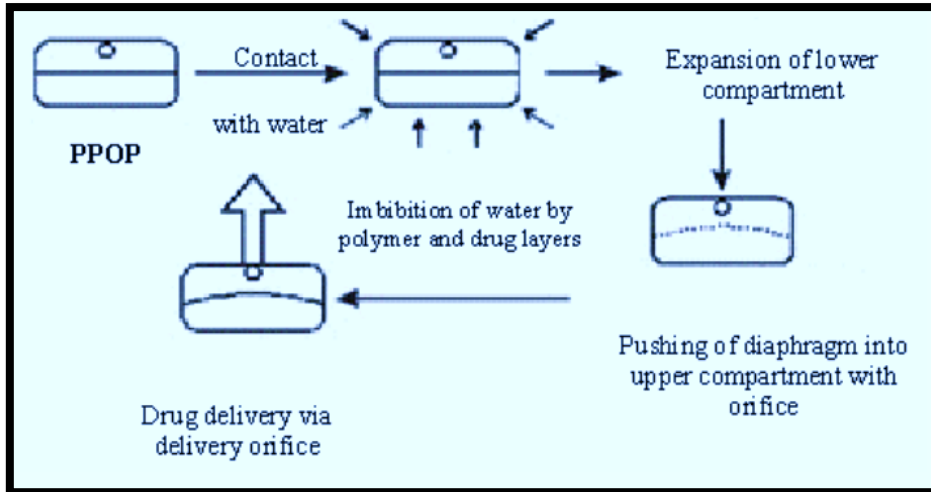


Figure 8: Illustration of Push–Pull Osmotic Pump–Mediated Controlled Drug Delivery

**Osmotic pump with a fixed-volume second chamber:**

In segmented osmotic assemblies, a non-expandable secondary compartment is incorporated to enhance therapeutic performance. This chamber functions either to dilute the released drug solution—minimising gastrointestinal irritation—or to enable the synchronised delivery of two active agents. Additionally, such designs expand the appropriateness of osmotic technology to sparingly soluble or insoluble drugs by optimising their release and bioavailability.<sup>xxii</sup>

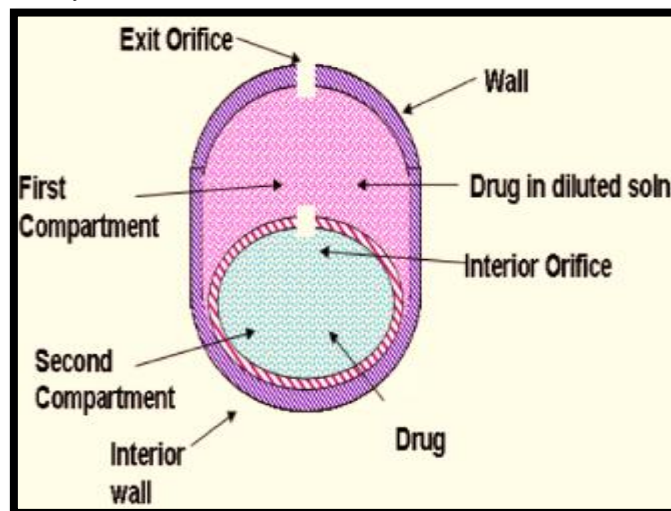


Figure 9: Schematic representation of an osmosis-based drug delivery device featuring a Non-Expanding Secondary Chamber.

**Modified Osmotic Pump  
Controlled Porosity Osmotic Pump**

The inner layer of a porosity-based osmosis-regulated tablet is encased within a semipermeable coating that permits drug elution through in-situ-generated pores. These pores are created by incorporating water-soluble pore-forming agents, by blending compounds, for example, NaCl, KCl, urea, or sucrose into the semipermeable coating. Upon exposure to aqueous media, these agents leach out, leaving behind pores that regulate and facilitate the timed liberation of the active ingredient.<sup>xxiv</sup>

©2025 The authors

This is an Open Access article

distributed under the terms of the Creative Commons Attribution (CC BY NC), which permits unrestricted use, distribution, and reproduction in any medium, as long as the original authors and source are cited. No permission is required from the authors or the publishers. (<https://creativecommons.org/licenses/by-nc/4.0/>)

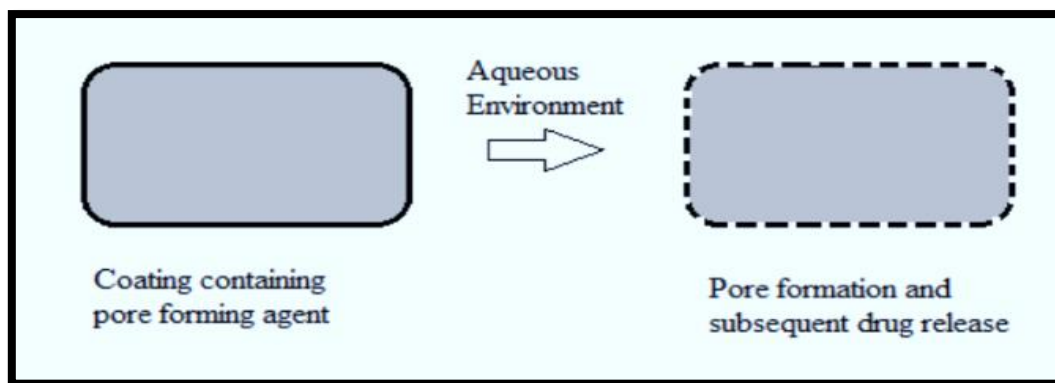


Figure 10: Representation of a Functional Mechanism of Controlled-Porosity Osmotic Pump.<sup>xxv</sup>

### Controlled Porosity Osmotic Pump

As an advancement in oral drug delivery, the CPOP was introduced as demonstrated in earlier reports of Zentner and associates (1991), Zentner and Rork, Appel and Zentner (1991), along with McClelland et al. Unlike conventional osmosis-based pumps, such a solid oral formulation represents a protected covered with a semipermeable barrier (SPM) embedded with excipients, leached pore-forming agents, eliminating the need for a pre-drilled delivery orifice. During operation, the pore formers dissolve upon contact with aqueous fluids, generating microporous channels through which the medication is dispensed. The mechanism of elution is driven by two key processes: (i) dissolution within the tablet core and (ii) release through membrane pores due to the synergistic effect of hydrostatic forces and permeation. When water permeates the SPM, the presence of osmotic agents, the drug itself, or other excipients generates internal pressure, which facilitates controlled delivery. Once pores are formed, the membrane allows simultaneous diffusion of water and solutes, resembling a sponge with interconnected tortuous channels of variable geometry.<sup>xxvi-xxvii</sup>

### Essential Ingredients of CPOP Tablets:

1. **Drug Core:** API & excipients; uniform release.
2. **Osmotic Agents:** Salts/sugars (NaCl, KCl, mannitol); create osmotic pressure.
3. **Wicking Agents:** Hydrophilic excipients (MCC, SLS, silica); aid hydration.
4. **Pore Formers:** Soluble additives (NaCl, sucrose, urea); form micropores.
5. **Semi-Permeable Membrane (SPM):** Cellulose acetate/ethyl cellulose; controls water entry, ensures zero-order release.
6. **Plasticisers:** PEG, triethyl citrate; improve flexibility, prevent cracking.
7. **Other Excipients:** Stabilisers, lubricants, surfactants, cyclodextrins; enhance stability & bioavailability.

### Solid Dispersion:

Solid dispersion involves dispersing drugs with low aqueous solubility in an inert hydrophilic carrier to improve dissolution properties and bioavailability. This system may be fabricated through different techniques, such as melting (fusion), evaporation of the solvent, or via a fusion of melting and solvent techniques. The formulation typically consists of a hydrophilic matrix that acts as the carrier and a hydrophobic drug that requires solubility enhancement.<sup>xxviii</sup>

### Preparation Methods of Solid Dispersions:

Solid dispersions are prepared to enhance solubility and bioavailability of poorly soluble drugs by dispersing them in hydrophilic carriers. Key methods include **fusion (melting)**, **solvent evaporation**, and **melting-solvent technique**, while advanced approaches such as **spray drying**, **lyophilisation**, **hot-melt extrusion**, **supercritical fluid processing**, and **co-precipitation** offer better control over particle size, stability, and reproducibility. The choice of method depends on drug properties, carrier characteristics, scalability, and intended application.<sup>xxix</sup>

©2025 The authors

This is an Open Access article

distributed under the terms of the Creative Commons Attribution (CC BY NC), which permits unrestricted use, distribution, and reproduction in any medium, as long as the original authors and source are cited. No permission is required from the authors or the publishers. (<https://creativecommons.org/licenses/by-nc/4.0/>)

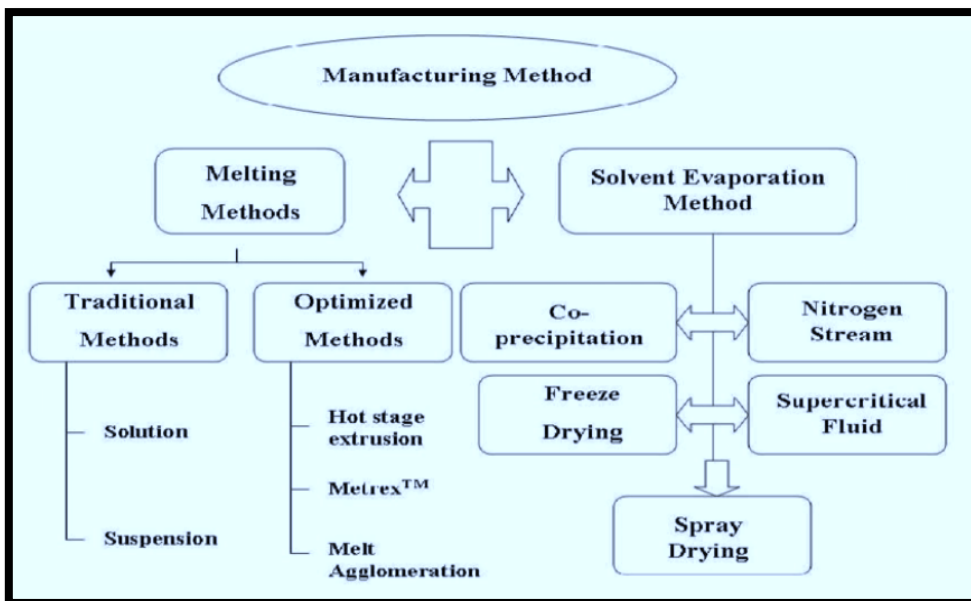


Figure 12: A schematic representation of different manufacturing methods for solid dispersions, including melting techniques (traditional and optimised) and solvent evaporation approaches.<sup>xxx</sup>

**Marketed oral osmotically driven products**

Drug	Brand
Doxazosin	Cardura CR
Methylphenidate	Concerta
Oxybutynin	Ditropan XL
Verapamil	Covera HS
Topiramate	Topamax
Glipizide	Glucotrol XL
Paliperidone	Invega
Pseudoephedrine	Allegra D 24h

**MATERIALS AND METHODS:**

Valacyclovir was obtained from Aurobindo Pharma Ltd., India. HPMC E5 LV was gifted by Colorcon Asia Pvt. Ltd., India. Sodium chloride was gifted by Merck Life Science, India. PVP K30 was procured from BASF India Ltd. Microcrystalline cellulose was procured from FMC Biopolymer/Signet Chem, India. Magnesium stearate and talc were procured from Loba Chemie Pvt. Ltd., India.

**EQUIPMENTS:**

A digital weighing balance (Shimadzu AUW220D), FTIR spectrophotometer (Bruker Alpha II), UV/Visible spectrophotometer (Elico, Ahmedabad), DSC (Shimadzu DSC-60, Japan), coating pan (VJ Instruments, New Delhi), Roche friabilator (Electro Lab, Mumbai), USP paddle-type II dissolution apparatus (Electrolab TDT-08L, Mumbai), SEM (Shimadzu DSC-60, Japan), stability chambers (Thermo Lab Scientific Equipment, Mumbai), and a 16-station rotary compression machine (Riddi, Ahmedabad) were used in the study.

**Preparation of Core Tablet of Valacyclovir:**

Valacyclovir core tablets were prepared by wet granulation. Sodium chloride, PVP K30, and HPMC E5 LV were blended (5 min) and sieved (No. 40). The blend was dampened with hydroalcoholic PVP K30 solution, granulated (No. 18), dried at 30–60 °C for 15–30 min, and sieved (No. 30). Talc (glidant) and magnesium stearate (lubricant) were added to the dried granules. The final blend was compressed into round tablets using a 16-station rotary press.<sup>xxxi-xxxiii</sup>

Tablet ingredients (mg)	FF1	FF2	FF3	FF4	FF5	FF6
Valacyclovir	250	250	250	250	250	250
HPMC E 5 LV	50	50	50	50	50	50
Sodium chloride	20	40	60	80	100	0
PVPK30	30	30	30	30	30	30

**©2025 The authors**

This is an Open Access article

distributed under the terms of the Creative Commons Attribution (CC BY NC), which permits unrestricted use, distribution, and reproduction in any medium, as long as the original authors and source are cited. No permission is required from the authors or the publishers.[\(https://creativecommons.org/licenses/by-nc/4.0/\)](https://creativecommons.org/licenses/by-nc/4.0/)

Micro Crystalline Cellulose	110	90	70	50	30	130
Magnesium stearate	10	10	10	10	10	10
Talc	10	10	10	10	10	10
Total weight (mg)	480	480	480	480	480	480

**Assessment of Pre-compression Parameters** <sup>xxxiv-xxxix</sup>

**Angle of Repose:** This method assesses powder flow by measuring the highest angle made by the powder's surface granular pile in addition to the flat area. Using the standard fixed funnel procedure, powder was dispensed into a funnel onto graph paper to form a conical pile. The heap's height (h) and radius (r) were recorded, and the angle of repose ( $\theta$ ) was computed using the formula:

$$\tan \theta = h / r$$

**Bulk Density:** The Bulk density is calculated and expressed in terms of powder mass over its bulk volume( $\text{g}/\text{cm}^3$ ) and is influenced by particle size, shape, and cohesiveness. To determine this, a 10 g portion of the powder blend was observed as it was placed in a 20 mL calibrated cylindrical vessel, which was formed without compaction, and the initial (untapped) volume ( $V_0$ ) was measured.

Bulk density was evaluated as:

$$\text{Bulk Density} = M / V_0$$

Where,

M = weight of sample,  $V_0$  = apparent volume of powder

**Tapped density:** Tapped density measures the proportion of powder mass relative to its volume after tapping until a constant volume is achieved. For measurement, the powder blend (10 g) was poured into a 20 mL cylinder and tapped until the final volume ( $V_t$ ) remained constant.

$$\text{Tapped Density} = \text{Tapped Volume (cm}^3\text{)} / \text{Weight of powder (g)}$$

**Measures of powder compressibility:** Compressibility percentage reflects the propensity to assess the powder's compressibility under pressure and is calculated using densities under bulk and tapped conditions. A lower value indicates better flow properties, as evidenced by the minimal change from bulk to tapped density, which is characteristic of powders with good flowability.

$$\text{Carr's Index} = [(\text{tap} - \text{b}) / \text{tap}] \times 100$$

Where, (b) = Bulk Density (Tap) = Tapped Density

**COATING OF CORE TABLETS:**

An **R&D coating pan (VJ Instruments, New Delhi, India)** with a rotating inclined pan and adjustable speed was used. Heated air ducts aided solvent evaporation, while an atomiser connected to a peristaltic pump and compressor sprayed fine droplets of coating solution onto the tablet bed.<sup>x1</sup>

**Preparation of Semipermeable Coating Solution:**

The coating formulation (FF1) was prepared by dissolving **cellulose acetate and PEG 400** in a suitable solvent with continuous stirring. **Sorbitol** was added as a pore-forming agent, and the solution was stirred for **12 hours** to obtain a transparent coating solution. Other formulations (FF2–FF6) were prepared similarly with varied ingredient proportions.<sup>xli-xlii</sup>

**Table 1 Composition of coating solution**

Formulation code	Cellulose acetate(g)	PEG 400 (mL)	PEG 600 (mL)	PEG 1500 (mL)	PEG 4000 (ml)	PEG 6000 (mL)	Sorbitol (g)	Acetone (mL)
FF1	6	2	0	0	0	0	0.4	300
FF2	6	0	2	0	0	0	0.8	300
FF3	6	0	0	2	0	0	1.2	300
FF4	6	0	0	0	2	0	1.6	300
FF5	6	2	0	0	0	2	2	300
FF6	6	0	0	0	0	0	2	300

©2025 The authors

This is an Open Access article

distributed under the terms of the Creative Commons Attribution (CC BY NC), which permits unrestricted use, distribution, and reproduction in any medium, as long as the original authors and source are cited. No permission is required from the authors or the publishers. (<https://creativecommons.org/licenses/by-nc/4.0/>)

**Post-compression Evaluation of Valacyclovir CPOP Tablets:**

The tablets underwent assessment for their weight, thickness, mechanical strength, friability, and drug content.

**Weight variation test:** To evaluate batch uniformity, twenty tablets were randomly selected and individually weighed using a digital balance. The mean tablet weight was calculated, and the percentage deviation of each tablet from the average was determined using the formula:

$$\% \text{deviation} = \frac{\text{individual weight} - \text{average weight}}{\text{average weight}} \times 100$$

**Tablet hardness:** Tablet hardness refers to the compressive force required to break a tablet along its diameter, reflecting its resistance to chipping, abrasion, and fracture during handling and storage. Six tablets from each formulation were randomly selected and tested using a Monsanto hardness tester. The mean hardness and standard deviation were calculated and documented.

**Thickness:** Thickness is a key parameter to ensure uniformity in size and appearance. The thickness of twenty coated tablets was tested with a digital micrometre, and the average value was recorded.

**Friability:** Tablet friability was assessed using a Roche friabilator to evaluate mechanical strength. Twenty pre-weighed tablets were rotated at 25 rpm for 4 minutes (100 revolutions). Post-run, tablets were reweighed, and the percentage weight loss was calculated to determine friability.

$$\% \text{Friability} = \frac{(W_1 - W_2)}{W_1} \times 100$$

**Drug content Analysis:** Ten tablets, equivalent to the mean tablet weight, were accurately weighed and finely powdered. A representative portion was transferred to a 100 mL volumetric flask containing 50 mL of distilled water and stirred until complete dissolution. The volume was adjusted to 100 mL with distilled water. Following suitable dilution, absorbance was measured at 304 nm using a UV-Visible spectrophotometer. Drug concentration was determined using a validated calibration curve (Luber et al., 1996).

$$\text{Drug Content (\%)} = \frac{\text{Amount of Drug Estimated}}{\text{Label Claim}} \times 100$$

**In vitro Drug Release Profile Studies:** The release profile of Valacyclovir from controlled porosity osmotic pump (CPOP) tablets was evaluated in triplicate using a USP Type II dissolution apparatus at 50 rpm and  $37 \pm 0.5$  °C. Tablets were initially immersed in 0.1 N HCl (pH 1.2) for 2 hours, followed by phosphate buffer (pH 7.4). At predetermined intervals, 5 mL aliquots were withdrawn, replaced with fresh medium, filtered, and analyzed spectrophotometrically at 304 nm. Drug release was quantified using a validated calibration curve and expressed as cumulative percentage release over time.

**Analysis of drug release kinetics:** The in vitro release profile of Valacyclovir from CPOP tablets was analyzed using various kinetic models to elucidate the mechanism of drug release. Non-linear models such as First-order and Korsmeyer–Peppas were applied to characterize the release behaviour. Regression analysis was performed, and the model exhibiting the highest correlation coefficient ( $R^2$ ) was considered the best fit for describing the release kinetics.

**Zero-order model:** Analysis of the drug release data was performed using the following equation to evaluate zero-order kinetics.

$$F = K_0 t$$

Where ‘F’ is the drug release at time ‘t’, ‘K<sub>0</sub>’ is the zero-order release rate constant.

**Higuchi release model:** The dissolution data were analyzed using the following equation to evaluate Higuchi release kinetics.

$$Q = kHt^{1/2}$$

Q = Amount of drug released at time t

H = Higuchi dissolution constant

t = Time

**©2025 The authors**

This is an Open Access article

distributed under the terms of the Creative Commons Attribution (CC BY NC), which permits unrestricted use, distribution, and reproduction in any medium, as long as the original authors and source are cited. No permission is required from the authors or the publishers. (<https://creativecommons.org/licenses/by-nc/4.0/>)

**Korsmeyer – Peppas’ power law kinetic model:** The drug release mechanism was analyzed using the Korsmeyer–Peppas model by plotting log (% drug released) against log (time), from which the release exponent (n) was determined.

$$(100-Q_t)^{1/3} = 100^{1/3} - K_{HC}.t$$

Where K = Hixson-Crowell rate constant

**First-order Model:** Although the process is complex to explain theoretically, the Korsmeyer–Peppas model has been widely applied to characterise the drug absorption and removal kinetics of specific drugs. This equation may also be employed to represent drug release patterns that follow first-order kinetics.

$$\text{Log } Q_t = \text{Log } Q_o + K t/2.303$$

Where,  $Q_t$  = Drug release measurement at time t, K = First-order release rate constant  
 $Q_o$  = Initial amount of drug in the solution.

**Effect of Osmogen Concentration:** CPOP tablets of Valacyclovir were formulated with varying concentrations of sodium chloride (0, 20, 40, 60, 80, and 100 mg per tablet; FSF6, FF1–FF5). Then, the tablets were analysed for testing the in vitro release profile via standard dissolution testing methods.

**Evaluation of Drug Release at Different pH Conditions:** To confirm the pH-independent behavior of the osmotic delivery system, in vitro release studies of the optimized Valacyclovir formulation were conducted using a USP Type II (paddle) apparatus at 50 rpm and 37 °C. Dissolution was performed in 900 mL of three media: 0.1 N HCl (pH 1.2), phosphate buffer pH 6.8, and phosphate buffer pH 7.4. At predetermined intervals, aliquots were withdrawn, replaced with fresh medium, and analyzed at 304 nm using UV–Visible spectrophotometry. Cumulative drug release data were plotted to assess the release profile across media.

**Table 2: Details of the Optimised Formulation for pH Study**

Ingredients (mg)	FF1	FF2	FF3	FF4	FF5	FF6
Valacyclovir	250	250	250	250	250	250
HPMC E 5 LV	50	50	50	50	50	50
Sodium chloride	20	40	60	80	100	0
PVPK30	30	30	30	30	30	30
Microcrystalline Cellulose	110	90	70	50	30	130
Magnesium stearate	10	10	10	10	10	10
Talc	10	10	10	10	10	10
<b>Total weight (mg)</b>	480	480	480	480	480	480

**Impact of Stirring Rate on Drug Release of Optimized Formulation:** To confirm that drug release from the osmotic system is independent of stirring speed, in vitro dissolution studies were performed on the optimized formulation using a USP Type II (paddle) apparatus at 50, 100, and 150 rpm. The release profiles were compared to assess the influence of agitational intensity on drug release behaviour.

**Table 3: Composition of Optimised Formulations for Agitational Intensity Study**

Ingredients (mg)	FF1	FF2	FF3	FF4	FF5	FF6
------------------	-----	-----	-----	-----	-----	-----

©2025 The authors

This is an Open Access article

distributed under the terms of the Creative Commons Attribution (CC BY NC), which permits unrestricted use, distribution, and reproduction in any medium, as long as the original authors and source are cited. No permission is required from the authors or the publishers. (<https://creativecommons.org/licenses/by-nc/4.0/>)

Valacyclovir	250	250	250	250	250	250
HPMC E 5 LV	50	50	50	50	50	50
Sodium chloride	20	40	60	80	100	0
PVPK30	30	30	30	30	30	30
Microcrystalline Cellulose	110	90	70	50	30	130
Magnesium stearate	10	10	10	10	10	10
Talc	10	10	10	10	10	10
<b>Total weight (mg)</b>	<b>480</b>	<b>480</b>	<b>480</b>	<b>480</b>	<b>480</b>	<b>480</b>

**Scanning Electron Microscopy Characterisation of the Membrane:** Coated tablets were examined for SEM-based surface analysis before and after dissolution to investigate the semipermeable layer structure and infer the drug release mechanism. (Sahoo et al., 2017).

**Accelerated Stability Studies:** Evaluation of Accelerated stability testing of the optimised or finalised formulation was executed following ICH guidelines. Formulated tablets were stored in airtight containers in a controlled stability chamber at  $40 \pm 2$  °C, 75 % relative humidity for 90 days. At regular intervals, Analyses were performed on the samples to assess appearance, drug quantification and in vitro release behaviour. (Dasankoppa et al., 2013).

## RESULTS AND DISCUSSION

**Pre-formulation Assessment:** Before developing the CPOP tablets, designed for controlled porosity, the identity and purity of the API must be confirmed through pre-formulation studies to ensure reliable and reproducible results. In this study, the drug was characterized using standard analytical methods to verify its structure and purity, and the findings are outlined in the subsequent sections.

**Physical and Sensory Properties:** The organoleptic properties of Valacyclovir hydrochloride are summarized in Table.

**Table 4: Organoleptic properties of Valacyclovir hydrochloride.**

Parameters	Observed
<b>Appearance</b>	Crystalline powder ranging from off-white to white
<b>Odor</b>	The drug exhibited no characteristic odour
<b>Taste</b>	Slightly bitter taste
<b>Texture</b>	Fine crystalline nature

**Melting Point Measurement:** The compound's (Valacyclovir hydrochloride) melting temperature was measured through the capillary method using a standard melting point device and is summarised in the Table 5.

**Table 5: Melting point of Valacyclovir hydrochloride by capillary method vs. literature values.**

Drug Name	Reported melting point	Observed
Vacyclovir hydrochloride	149°C -	150–152 °C

**Solubility Studies:** Valacyclovir HCl showed low solubility in acidic medium (8.4 mg/mL at pH 1.2), which

©2025 The authors

This is an Open Access article

distributed under the terms of the Creative Commons Attribution (CC BY NC), which permits unrestricted use, distribution, and reproduction in any medium, as long as the original authors and source are cited. No permission is required from the authors or the publishers. (<https://creativecommons.org/licenses/by-nc/4.0/>)

increased with pH, reaching 43.5 mg/mL at pH 11 due to ionisation at higher pH. The solubility assessment results are presented in Table 6 .

Table 6: Solubility assessment of Valacyclovir (n=3)

Solvents	Solubility mg/mL
0.1N HCl (pH 1.2)	8.4±0.21
Phosphate buffer (pH 6.8)	16.1±1.59
Double-distilled water (pH 7.0)	23.7±0.39
Phosphate buffer (pH 7.2)	27.7±0.65
pH 7.4 Phosphate buffer	33.8±1.46
0.1N NaOH (pH 11.0)	43.5±0.81

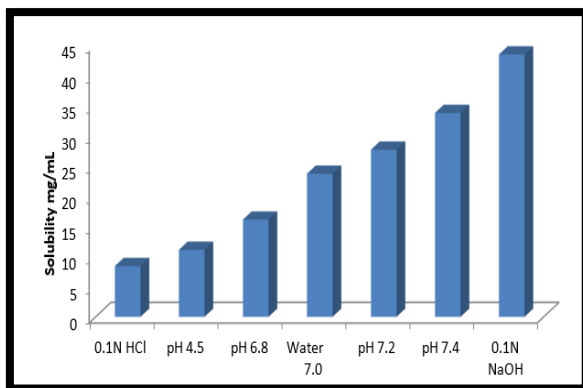


Figure 13: Solubility Profile of Valacyclovir

UV spectroscopic study:

**Determination of Maximum Absorbance Wavelength ( $\lambda_{max}$ ) of Valacyclovir in 1.2 N HCl:** The  $\lambda_{max}$  of Valacyclovir in 0.1 N HCl buffer (pH 1.2) was determined via UV-Visible spectroscopy. The absorption spectrum (Figure 6.2) showed a characteristic maximum at 252.8 nm, and the corresponding absorbance. Table 7 presents the experimental results.

Table 7: UV absorbance of Valacyclovir in 0.1 N HCl buffer (pH 1.2)

Drug Name	Observed lambda max
Valacyclovir	252.8nm

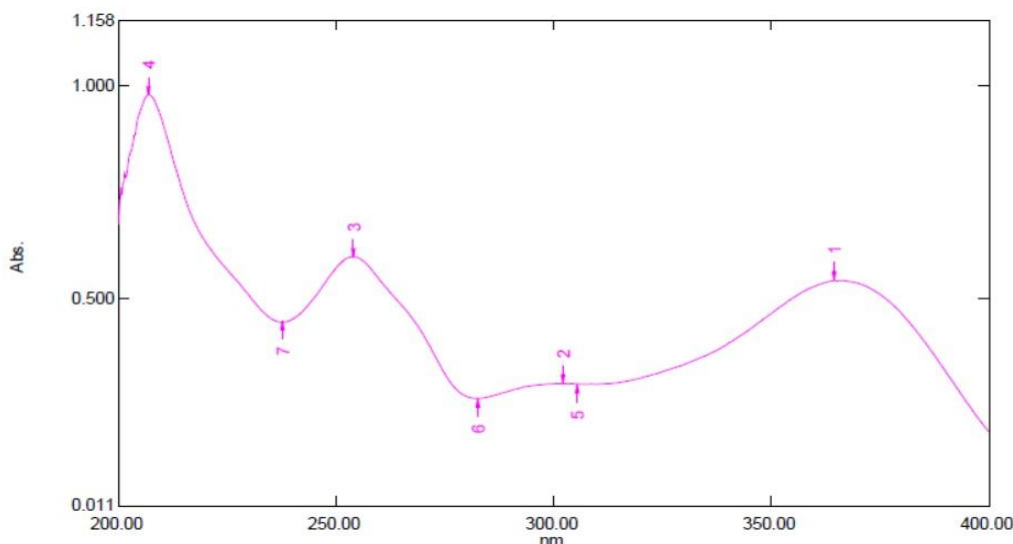


Figure 14: UV absorption spectrum of Valacyclovir showing  $\lambda_{max}$  at 252.8 nm in 0.1 N HCl buffer (pH 1.2)

**Determination of Maximum Absorbance Wavelength ( $\lambda_{max}$ ) of Valacyclovir in Phosphate buffer pH 6.8:**

©2025 The authors

This is an Open Access article

distributed under the terms of the Creative Commons Attribution (CC BY NC), which permits unrestricted use, distribution, and reproduction in any medium, as long as the original authors and source are cited. No permission is required from the authors or the publishers. (<https://creativecommons.org/licenses/by-nc/4.0/>)

The absorption spectrum (Figure 15) showed a distinct maximum at 252 nm, with the associated absorbance data listed in Table 8.

Table 8: UV absorbance of Valacyclovir in phosphate buffer (pH 6.8)

Drug Name	Observed lambda max
Valacyclovir	252nm

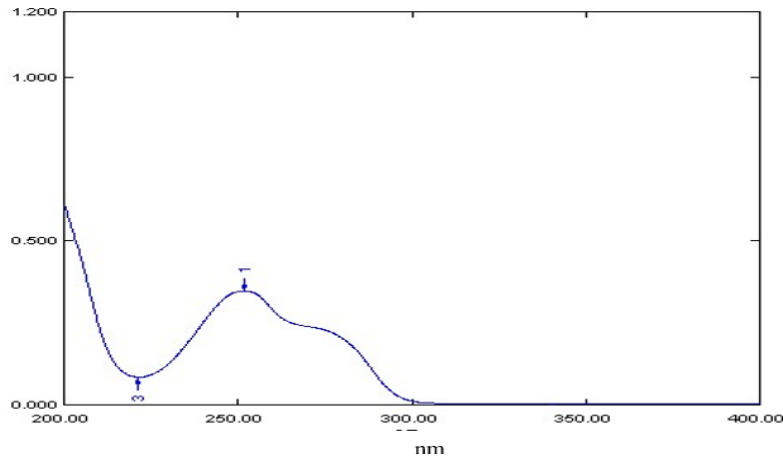


Figure 15: Valacyclovir absorption peak at 252.8 nm in Phosphate buffer [ pH 6.8]

**Determination of Maximum Absorbance Wavelength ( $\lambda_{max}$ ) of Valacyclovir in Phosphate buffer pH 7.4:** The absorption spectrum (Figure 16) exhibited a distinct peak at 260 nm. Corresponding absorbance values across concentrations are tabulated in Table 9.

Table 9: UV absorbance profile of Valacyclovir in buffer (pH 7.4)

Drug Name	Observed lambda max
Valacyclovir	260nm

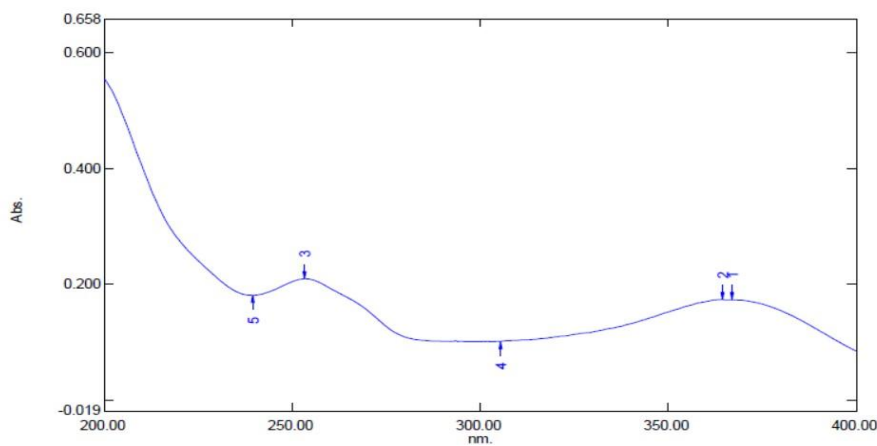


Figure 16: The UV absorption spectrum of Valacyclovir exhibited a maximum absorbance ( $\lambda_{max}$ ) at 260 nm in phosphate buffer (pH 7.4).

**Development of Standard Calibration Curve :**

**Standard Calibration Curve of Valacyclovir in Different Media:**

Standard calibration curves of Valacyclovir were constructed in distilled water, 0.1 N HCl (pH 1.2), phosphate buffer pH 6.8, and phosphate buffer pH 7.4. Concentration ranges were 5–30  $\mu\text{g/mL}$  depending on medium. All curves showed excellent linearity with regression equations and correlation coefficients close to 1, confirming the reliability of the method for quantitative analysis.

- Distilled water:  $y = 0.036x + 0.002$  ( $R^2 = 0.997$ )

©2025 The authors

This is an Open Access article

distributed under the terms of the Creative Commons Attribution (CC BY NC), which permits unrestricted use, distribution, and reproduction in any medium, as long as the original authors and source are cited. No permission is required from the authors or the publishers. (<https://creativecommons.org/licenses/by-nc/4.0/>)

- 0.1 N HCl (pH 1.2):  $y = 0.040x + 0.0032$  ( $R^2 = 0.999$ )
- Phosphate buffer pH 6.8:  $y = 0.030x + 0.0021$  ( $R^2 = 0.998$ )
- Phosphate buffer pH 7.4:  $y = 0.038x + 0.002$  ( $R^2 = 0.998$ )

Table 10: Combined Interpretation of Calibration Curves of Valacyclovir

Concentration (µg/mL)	Absorbance in Water (304 nm)	Absorbance in 0.1 N HCl (252.8 nm)	Absorbance in Phosphate Buffer pH 6.8 (304 nm)	Absorbance in Phosphate Buffer pH 7.4 (260 nm)
5	0.235	0.215	0.150	0.190
10	0.424	0.433	0.274	0.392
15	0.574	0.645	0.476	0.591
20	0.729	0.863	0.610	0.775
25	0.906	0.994	0.748	0.950
30	—	—	0.955	—

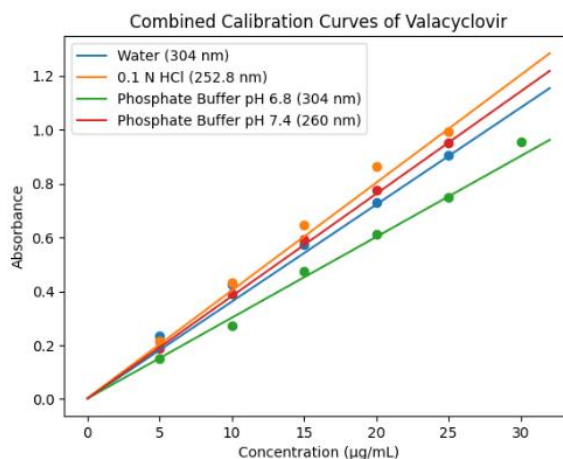


Figure 17: Analytical calibration graph of Valacyclovir

**Drug- Excipient Compatibility Analysis:**

**Differential Scanning Calorimetry (DSC) of pure drug:** The thermogram of pure Valacyclovir revealed a pronounced endothermic peak at 103.18 °C (onset: 96.32 °C; end: 108.12 °C;  $\Delta H = 1081.1580$  J/g), indicative of its melting temperature and confirms its crystalline form and purity.

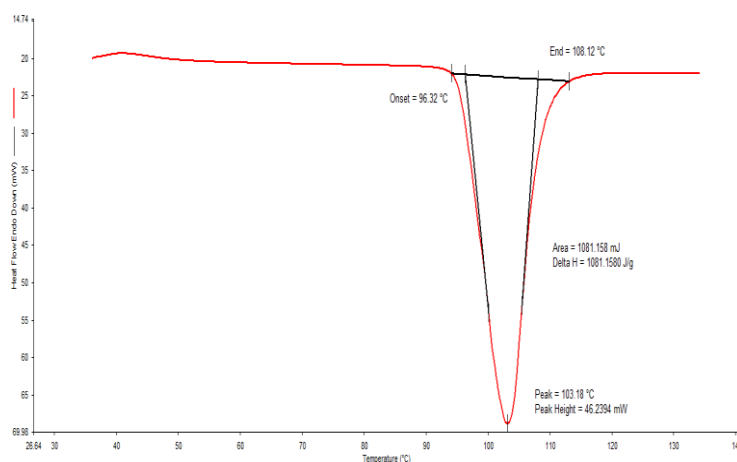


Figure 18: DSC thermogram of valacyclovir

**DSC of Optimized Formulation’s Physical Mixture (FF5):** Thermal analysis of the physical blend of the optimized formulation (API + PVP K30 + HPMC E5 LV) presented a typical drug peak at 101.37 °C, along with additional peaks at 130 °C and 269.25 °C, attributable to the excipients. The manifestation of the drug’s melting peak in the mixture without a notable shift or disappearance indicates no major physicochemical interaction, suggesting compatibility between valacyclovir and the selected excipients.

©2025 The authors

This is an Open Access article

distributed under the terms of the Creative Commons Attribution (CC BY NC), which permits unrestricted use, distribution, and reproduction in any medium, as long as the original authors and source are cited. No permission is required from the authors or the publishers. (<https://creativecommons.org/licenses/by-nc/4.0/>)

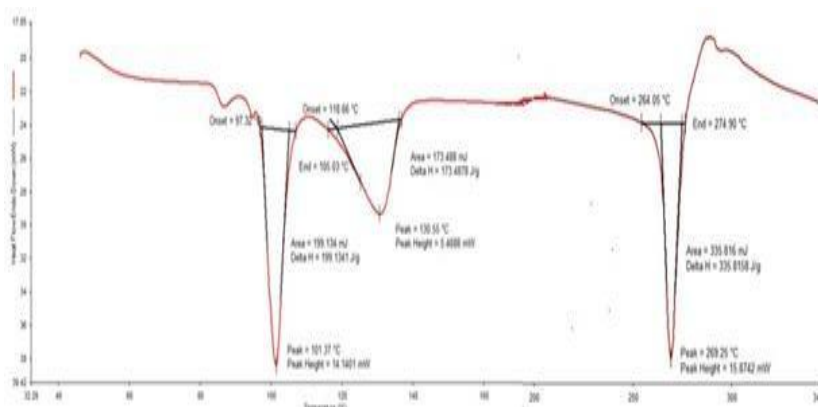


Figure 19: DSC curve representing the physical mixture of the optimized formulation (FF5)

**FTIR Characterisation**

**FTIR of Pure Drug:** The characteristic FTIR spectrum of valacyclovir displayed specific spectral peaks representing its functional groups. A band at 1421.51 cm<sup>-1</sup> was assigned to C–O–H bending, while peaks at 1547.33 cm<sup>-1</sup> and 1654.83 cm<sup>-1</sup> were assigned to C=C (aromatic stretching) and C=N stretching, respectively. The spectrum also displayed C–H stretching vibrations at 3070.25 cm<sup>-1</sup> (aromatic ring) and 2865.65 cm<sup>-1</sup> (aliphatic), along with a peak at 1232.75 cm<sup>-1</sup> corresponding to C–N stretching. The results align with values reported in the literature, confirming the structural integrity of valacyclovir.

Table 11: FTIR spectral interpretation of Pure Valacyclovir

S.NO	Experimental Peak[cm <sup>-1</sup> ]	Reported Peak[cm <sup>-1</sup> ]	Identified Functional Group
1.	1421.51	1440–1220	C–O–H bending
2.	1547.33	1650–1550	C=C stretching (aromatic)
3.	1654.83	1600–1500	C=N stretching
4.	3070.25	3100–3000	C–H stretching (aromatic ring)
5.	2865.65	2900–2800	C–H stretching (aliphatic)
6.	1232.75	1340–1250	C–N stretching

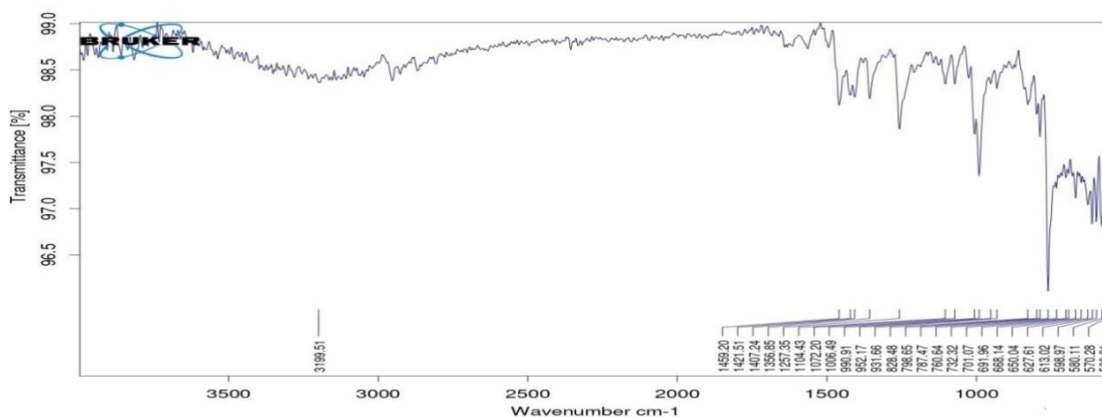


Figure 20: FTIR Spectra of Valacyclovir

**FTIR Analysis of Physical Mixture (FF5):** Infrared spectral examination of the optimised formulation (FF5) was recorded to assess any possible interactions between Valacyclovir and the selected excipients (HPMC E 5 LV, sodium chloride, PVPK30, microcrystalline cellulose, magnesium stearate, talc). The observed peaks at 1236.50, 1537.36, 1652.38, 3074.52, 2863.56, and 1222.65 cm<sup>-1</sup> correspond to the reported characteristic peaks of Valacyclovir at 1421.51, 1547.33, 1654.83, 3070.25, 2865.65, and 1232.75 cm<sup>-1</sup>, associated with C–O–H bending. The characteristic peaks for C=C (aromatic), C=N, C–H (aromatic), C–H (aliphatic), and C–O–C stretching were detected in the physical mixture, indicating no significant interdependence between valacyclovir and the excipients. Minor shifts may result from hydrogen bonding or physical mixing, confirming compatibility in FF5.

©2025 The authors

This is an Open Access article

distributed under the terms of the Creative Commons Attribution (CC BY NC), which permits unrestricted use, distribution, and reproduction in any medium, as long as the original authors and source are cited. No permission is required from the authors or the publishers. (<https://creativecommons.org/licenses/by-nc/4.0/>)

Table 12: FTIR spectral interpretation of Physical Mixture (FF5)

S.NO	Experimental Peak[cm <sup>-1</sup> ]	Reported Peak[cm <sup>-1</sup> ]	Identified Functional Group
1.	1236.50	1421.51	C–O–H bending (alcohol/hydroxyl)
2.	1537.36	1547.33	C=C stretching (aromatic ring)
3.	1652.38	1654.83	C=N stretching
4.	3074.52	3070.25	C–H stretching (aromatic)
5.	2863.56	2865.65	C–H stretching (aliphatic)
6.	1222.65	1232.75	C–O–C stretching

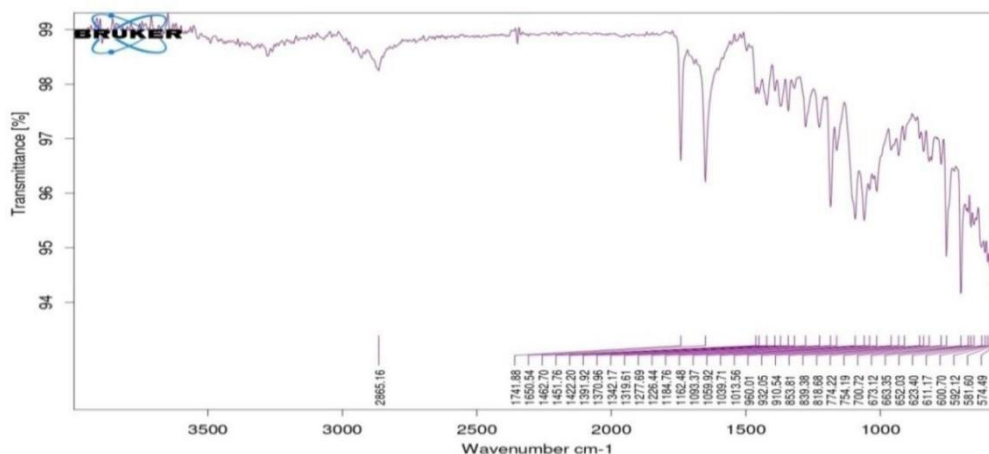


Figure 21: FTIR spectrum of the physical mixture (FF5)

**Assessment of Pre-compression Characteristics of powder blend:**

**Flow Property Evaluation**

The angle of repose, bulk density, tapped density, Carr’s index, and Hausner’s ratio of formulations FF1–FF6 are summarised in Table 13. All formulations showed acceptable flow and compressibility, with FF5 exhibiting the most favourable values, confirming excellent flowability and supporting its selection as the optimised formulation.

Table 13: Flow Property Evaluation of Formulations (FF1–FF6)

Formulation	Angle of Repose (°)	Bulk Density (g/cm <sup>3</sup> )	Tapped Density (g/cm <sup>3</sup> )	Carr’s Index (%)	Hausner’s Ratio
FF1	31.12	0.517	0.625	14.88	1.174
FF2	29.08	0.499	0.642	15.75	1.187
FF3	29.55	0.504	0.619	14.05	1.190
FF4	27.40	0.526	0.621	18.10	1.310
FF5	<b>23.68</b>	<b>0.508</b>	<b>0.627</b>	<b>13.05</b>	<b>1.110</b>
FF6	26.26	0.509	0.609	16.98	1.125

**Post-compression Evaluation of Valacyclovir CPOP Tablets:** Physicochemical evaluation of the developed tablets is given below within pharmacopoeial limits:

**Tablet Evaluation Parameters:**

The weight variation, thickness, and friability of formulations FF1–FF6 are summarised in Table 14. All batches showed acceptable uniformity and mechanical strength, with FF5 exhibiting the most favourable values (weight 399.06 mg, thickness 3.79 mm, friability 0.26%), confirming its suitability as the optimised formulation.

Table 14: Weight, Thickness, and Friability of Formulations (FF1–FF6)

Formulation	Weight (mg)	Thickness (mm)	Friability (%)
FF1	397.50	3.76	0.69
FF2	401.02	3.90	0.28
FF3	402.07	3.88	0.47
FF4	397.02	3.81	0.53
FF5	<b>399.06</b>	<b>3.79</b>	<b>0.26</b>
FF6	398.00	3.92	0.75

**In vitro release Profile studies:** Valacyclovir release from CPOP tablets was evaluated using a USP paddle

©2025 The authors

This is an Open Access article

distributed under the terms of the Creative Commons Attribution (CC BY NC), which permits unrestricted use, distribution, and reproduction in any medium, as long as the original authors and source are cited. No permission is required from the authors or the publishers. (<https://creativecommons.org/licenses/by-nc/4.0/>)

apparatus. After 24 h, FF1–FF4, FF5, and FSF6 released 84.9%, 86.3%, 87.1%, 90.1%, 99.2%, and 80.3%, respectively. The highest release in **FF5** was attributed to its higher osmogen (NaCl 100 mg) and polymer (HPMC E5 LV 50 mg), while FSF6 showed the lowest due to absence of osmogen. These findings confirm that drug release is governed by osmotic pressure and membrane composition, with **FF5 optimised for controlled delivery**.

Table 15: In vitro drug release of various valacyclovir CPOP formulations (values expressed as mean cumulative % drug release ± SD)

Time (hrs)	Percent cumulative release of the drug					
	FF1	FF2	FF3	FF4	FF5	FSF6
0	0	0	0	0	0	0
1	3.56±1.4	4.1±1.9	5.2±1.6	6.4±1.2	<b>9.8±1.4</b>	2.4±1.2
2	7.56±1.1	9.6±2.4	11.2±1.8	13.2±1.8	<b>16.03±1.6</b>	5.7±1.7
3	10.42±1.6	12.5±1.5	14.6±1.0	15.6±1.0	<b>20.3±1.1</b>	9.4±1.6
4	16.54±1.2	20.1±2.1	23.3±1.2	25.6±1.2	<b>28.2±1.3</b>	14.5±1.1
6	23.54±1.1	26.5±1.1	28.03±1.4	31.2±1.2	<b>37.2±1.6</b>	21.2±1.5
8	31.25±1.3	34.2±1.7	36.01±1.7	42.6±1.7	<b>49.3±2.1</b>	28.2±1.1
10	40.25±1.5	43.2±1.1	46.08±1.3	50.2±1.0	<b>54.01±1.4</b>	38.6±1.6
12	50.26±1.4	51.06±1.5	54.06±1.2	59.5±1.4	<b>63.2±1.6</b>	48.1±1.0
16	65.42±1.2	68.4±1.4	72.01±1.0	74.8±1.9	<b>78.9±1.1</b>	63.4±1.9
20	78.46±1.0	79.9±1.7	81.2±1.2	85.1±1.3	<b>89.2±1.4</b>	71.01±1.1
24	84.59±1.1	86.3±1.2	87.12±1.4	90.10±1.2	<b>100.1±1.6</b>	80.3±1.3

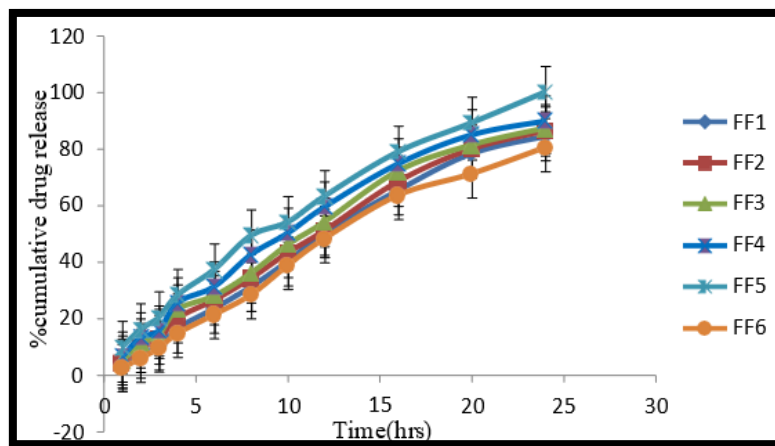


Figure 22: Drug release profiles of Valacyclovir CPOP formulations in vitro.

**Analysis of Drug Release Kinetics of dissolution data:** Drug release from CPOP tablets followed the **Zero-order model** ( $R^2 = 0.992–0.999$ ), confirming concentration-independent release. FF1–FF4 and FSF6 showed good Zero-order fitting with supportive Higuchi and Hixson–Crowell correlations, while **FF5 exhibited the strongest Zero-order fit ( $R^2 = 0.9991$ )** along with high First-order and Hixson–Crowell values, establishing it as the **optimised formulation**.

Table 16: In-vitro drug kinetics of various Valacyclovir CPOP Tablets

Model	R <sup>2</sup> Values
Zero Order	0.9991
First Order	0.9941
Higuchi	0.9173
Korsmeyer–Peppas	0.7093
Hixson–Crowell	0.995

©2025 The authors

This is an Open Access article

distributed under the terms of the Creative Commons Attribution (CC BY NC), which permits unrestricted use, distribution, and reproduction in any medium, as long as the original authors and source are cited. No permission is required from the authors or the publishers. (<https://creativecommons.org/licenses/by-nc/4.0/>)

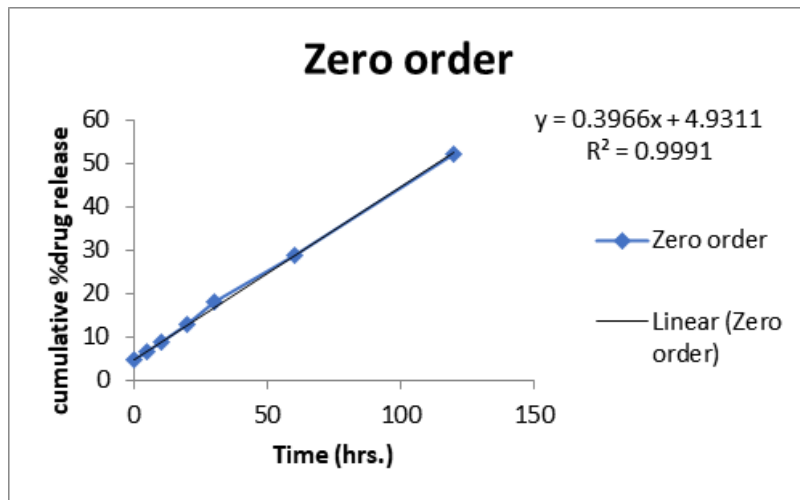


Figure 23: Representing the Zero-order model (FF5)



Figure 24: Representing the First-order model (FF5)

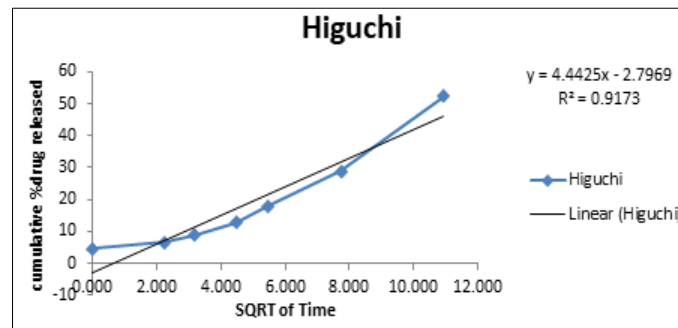
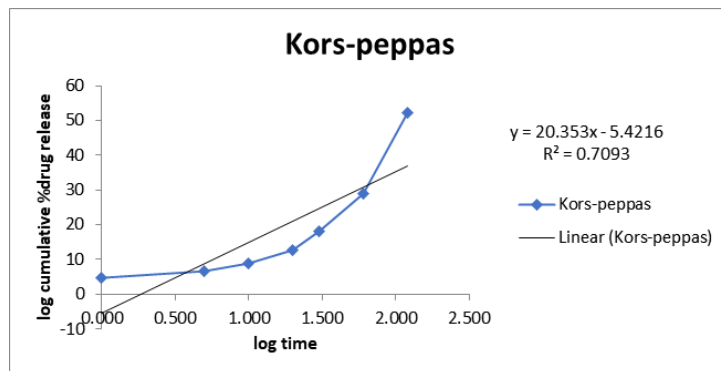


Figure 25: Representing the Higuchi model (FF5)



©2025 The authors

This is an Open Access article

distributed under the terms of the Creative Commons Attribution (CC BY NC), which permits unrestricted use, distribution, and reproduction in any medium, as long as the original authors and source are cited. No permission is required from the authors or the publishers. (<https://creativecommons.org/licenses/by-nc/4.0/>)

Figure 26: Representing the Kors-peppas model (FF5)

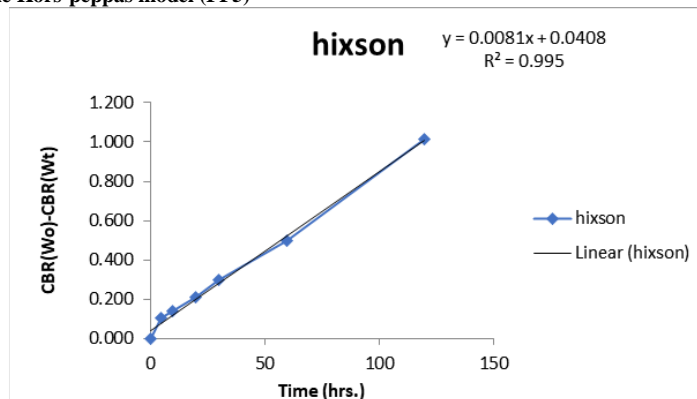


Figure 27: Representing the Kors-peppas model (FF5)

**Evaluation of Drug Release at Different pH Conditions:** The osmotic release mechanism enables drug delivery regardless of the composition of the surrounding medium pH. The FF5 formulation exhibited consistent cumulative drug release across different pH buffers. The release profile is presented in Table 2.13 and Figure 2.11, indicating that valacyclovir release from FF5 CPOP tablets is unaffected by gastrointestinal pH, demonstrating the system’s robustness.

Table 17: Influence of medium pH on the dissolution of FF5 CPOP tablets

Time (hrs)	% cumulative drug release		
	pH 0.1 N HCl	Phosphate Buffer at pH6.8	Phosphate Buffer at pH 7.4
0	0	0	0
1	9.1±1.5	9.8±1.4	9.4±1.3
2	16.01±1.2	16.03±1.6	16.02±1.1
3	20.1±1.3	20.3±1.1	20.2±1.3
4	27.8±1.3	28.2±1.3	28.0±1.0
6	36.9±1.2	37.2±1.6	37.1±1.4
8	49.1±1.1	49.3±2.1	48.9±1.6
10	53.8±1.6	54.01±1.4	53.10±1.1
12	61.0±1.5	63.2±1.6	60.01±1.3
16	78.2±1.1	78.9±1.1	78.5±1.2
20	88.9±1.0	89.2±1.4	89.0±1.1
24	99.2±1.5	100.1±1.6	100.1±1.0

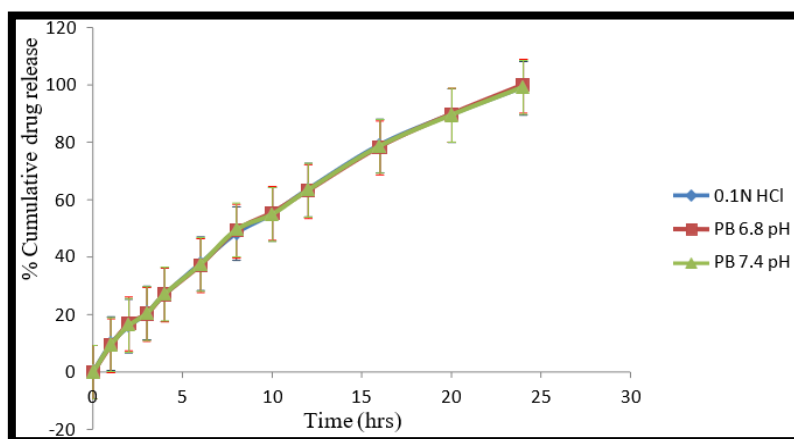


Figure 28: Dissolution Profile of FF5 CPOP Tablets at Different pH Conditions (n = 3)

**Impact of Stirring Rate on Drug Release of Optimised Formulation (FF5):** In vitro evaluation of Controlled drug release behaviour of the optimised batch FF5 formulation was not influenced by agitational speed. These findings indicate that hydrodynamic conditions have minimal effect on the release of the drug from the

©2025 The authors

This is an Open Access article

distributed under the terms of the Creative Commons Attribution (CC BY NC), which permits unrestricted use, distribution, and reproduction in any medium, as long as the original authors and source are cited. No permission is required from the authors or the publishers. (<https://creativecommons.org/licenses/by-nc/4.0/>)

formulation. The percentage cumulative drug release profile of FF5 is presented in **Table 18** and **Figure 29**

**Table 18: Influence of paddle rotation speed on FF5 drug release**

Time (hrs)	Cumulative Release of Drug (%)		
	50 rpm	100rpm	150rpm
0	0	0	0
1	9.9±1.6	9.3±1.3	9.6±1.0
2	16.01±1.4	16.9±0.1	16.3±0.3
3	20.6±1.2	20.2±1.3	20.4±1.1
4	27.0±1.0	27.01±1.1	27.2±1.5
6	37.8±1.6	37.2±1.3	37.5±1.0
8	48.3±1.1	49.2±1.5	49.5±1.3
10	55.01±1.2	55.4±1.0	54.9±1.5
12	63.5±1.5	63.0±1.1	63.3±1.2
16	78.9±1.1	78.2±1.0	78.6±1.1
20	89.5±1.4	89.6±1.1	89.4±1.5
24	99.01±1.6	99.7±1.0	99.1±1.3

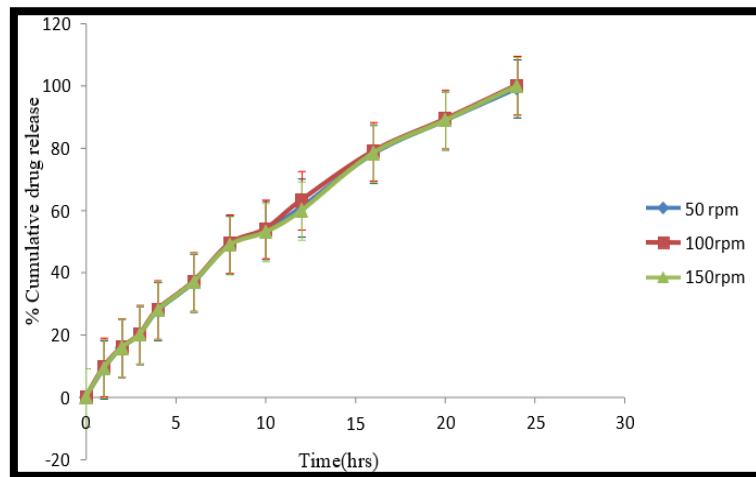
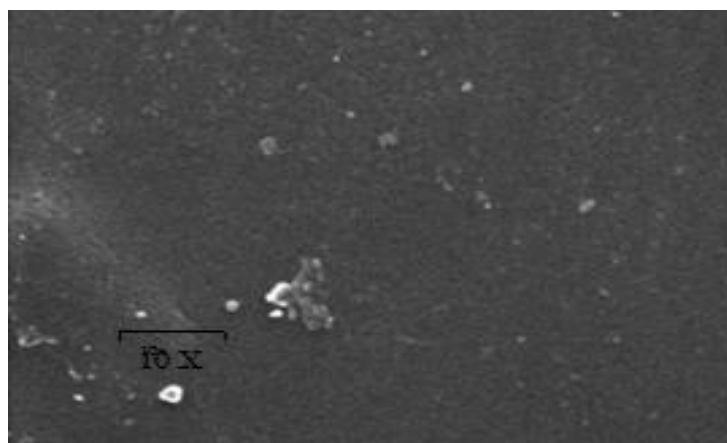


**Figure 29: In Vitro Formulation Release of FF5 at Varying RPM (n = 3)**

**Scanning Electron Microscopy (SEM) Characterisation of the membrane:** SEM revealed smooth, non-porous tablet surfaces before dissolution, while pores (1–50 μm) formed after 24 h, acting as drug release channels. The semi-permeable coating remained intact, and in FF5 sorbitol and PEG 400/6000 functioned as pore-forming and flux-regulating agents, enabling controlled release

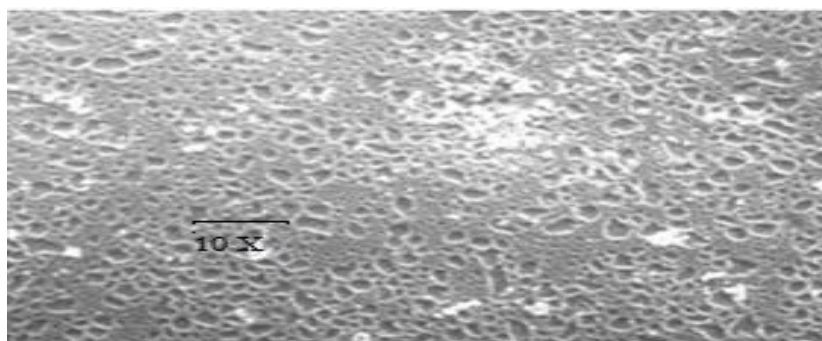


**(a) prior to dissolution**

©2025 The authors

This is an Open Access article

distributed under the terms of the Creative Commons Attribution (CC BY NC), which permits unrestricted use, distribution, and reproduction in any medium, as long as the original authors and source are cited. No permission is required from the authors or the publishers. (<https://creativecommons.org/licenses/by-nc/4.0/>)



(b) post-dissolution

Figure 30. SEM images of semi-permeable membrane (a) before dissolution and (b) post-dissolution

**Accelerated Stability Studies:** The finalised formulation FF5 was assessed for stability under forced degradation conditions over a period of three months under specified storage conditions. The formulation was assessed for periodic evaluation of tablet appearance, mechanical strength, friability, drug content, and dissolution profile. No substantial observed differences included any of these parameters throughout the study period. The tablets retained their original appearance, mechanical strength, and drug content, together with the “in vitro observations remained consistent, indicating that the FF5 formulation is stable and maintains its performance over time.

## CONCLUSION:

The Valacyclovir CPOP tablets were successfully formulated and evaluated. Sodium chloride, Sorbitol, and HPMC E 5 LV were employed as osmogen, pore-forming agent, and polymer, respectively. Thermal and IR spectroscopy studies validated the evaluation regarding interactions between valacyclovir and the selected excipients. In vitro experiments provided evidence that the amounts of osmogen and polymer in the core, along with the pore-forming and flux-controlling agents in the coating, are key factors in regulating drug release from the CPOP tablets. The FF5 formulation exhibited zero-order release, providing a constant and sustained active ingredient release profile.

Pharmacokinetic studies conducted in rabbits showed a distinct elevation of the FF5 formulation against the marketed sustained-release product (Penvir SR). Bioavailability of the test product was noted to be 1.90, confirming the superior performance of the optimized valacyclovir CPOP tablets.

## REFERENCES:

- i. P. Upadhyay, K. Nayak, K. Patel, J. Patel, S. Shah, and J. Deshpande, “Formulation development, optimization, and evaluation of sustained release tablet of valacyclovir hydrochloride by combined approach of floating and swelling for better gastric retention,” *Drug Deliv. Transl. Res.*, vol. 4, no. 5–6, pp. 452–464, 2014, doi: 10.1007/s13346-014-0207-x.
- ii. R. Narendra, S. Pavan, D. Sravani, M. Sumanta, and S. Ganapathi, “Development and validation of new analytical methods for the estimation of Valacyclovir hydrochloride in pharmaceutical dosage form,” *Der Pharm. Lett.*, vol. 8, no. 1, pp. 296–303, 2016.
- iii. B. P. Rao, M. Geetha, N. Purushothama, and U. Sanki, “Optimization and development of swellable controlled porosity osmotic pump tablet for theophylline,” *Trop. J. Pharm. Res.*, vol. 8, no. 3, pp. 247–255, 2009, doi: 10.4314/tjpr.v8i3.44541.
- iv. P. Kumar, S. Singh, and B. Mishra, “Development and biopharmaceutical evaluation of extended release formulation of tramadol hydrochloride based on osmotic technology,” *Acta Pharm.*, vol. 59, no. 1, pp. 15–30, 2009, doi: 10.2478/v10007-009-0010-2.
- v. A. Ali and O. M. Sayed, “Development and characterization of ketorolac tromethamine osmotic pump tablets,” *J. Drug Deliv. Sci. Technol.*, vol. 23, no. 3, pp. 275–281, 2013, doi: 10.1016/S1773-2247(13)50041-4.
- vi. Mabelele, “基因的改变 NIH Public Access,” *Bone*, vol. 23, no. 1, pp. 1–7, 2008, doi: 10.1016/j.antiviral.2013.08.007.Osmotic.
- vii. R. K. Verma, D. M. Krishna, and S. Garg, “Formulation aspects in the development of osmotically controlled oral drug delivery systems,” *J. Control. Release*, vol. 79, no. 1–3, pp. 7–27, 2002, doi: 10.1016/S0168-3659(01)00550-8.
- viii. Prasanna N., Srilatha C., and Subrahmanyam C. V. S., “Osmotic Controlled Release Oral Delivery System: An Overview,” *Int. J. Pharm. Sci*, vol. 2, no. 3, pp. 530–558, 2024, doi: 10.5281/zenodo.10810393.
- ix. U. Kumar, S. R. K. U. K. G., and H. K. M., “World Journal of Pharmaceutical research MICROPOROUS OSMOTIC TABLETS OF RIVASTIGMINE,” vol. 3, no. 2, pp. 2493–2503, 2014.
- x. R. Bhanushali, R. Wakode, and A. Bajaj, “Monolithic osmotic tablets for controlled delivery of antihypertensive drug,” *J. Pharm. Innov.*, vol. 4, no. 2, pp. 63–70, 2009, doi: 10.1007/s12247-009-9055-5.
- xi. S. Tuntikulwattana, N. Sinchaipanid, W. Ketjinda, D. B. Williams, and A. Mitrevej, “Fabrication of chitosanpolyacrylic acid complexes as polymeric osmogens for swellable micro/nanoporous osmotic pumps,” *Drug Dev. Ind. Pharm.*, vol. 37, no. 8, pp. 926–933, 2011, doi: 10.3109/03639045.2010.550300.
- xii. X. Cheng, M. Sun, Y. Gao, F. Cao, and G. Zhai, “Design and evaluation of osmotic pump-based controlled release system of Ambroxol Hydrochloride,” *Pharm. Dev. Technol.*, vol. 16, no. 4, pp. 392–399, 2011, doi: 10.3109/10837451003774385.
- xiii. Abd-Elbary, M. I. Tadros, and A. A. Alaa-Eldin, “Development and in vitro/in vivo evaluation of etodolac controlled porosity osmotic pump tablets,” *AAPS PharmSciTech*, vol. 12, no. 2, pp. 485–495, 2011, doi: 10.1208/s12249-011-9608-z.

## ©2025 The authors

This is an Open Access article

distributed under the terms of the Creative Commons Attribution (CC BY NC), which permits unrestricted use, distribution, and reproduction in any medium, as long as the original authors and source are cited. No permission is required from the authors or the publishers. (<https://creativecommons.org/licenses/by-nc/4.0/>)

- xiv. W.-J. Xu, N. Li, and C. Gao, "Preparation of controlled porosity osmotic pump tablets for salvianolic acid and optimization of the formulation using an artificial neural network method," *Acta Pharm. Sin. B*, vol. 1, no. 1, pp. 64–70, 2011, doi: 10.1016/j.apsb.2011.04.002.
- xv. Z. Zhao, C. Wu, Y. Zhao, Y. Hao, Y. Liu, and W. Zhao, "Development of an oral push-pull osmotic pump of fenofibrate-loaded mesoporous silica nanoparticles," *Int. J. Nanomedicine*, vol. 10, pp. 1691–1701, 2015, doi: 10.2147/IJN.S76755.
- xvi. C. K. Sahoo, N. K. Sahoo, S. R. M. Rao, M. Sudhakar, and K. Satyanarayana, "A review on controlled porosity osmotic pump tablets and its evaluation," *Bull. Fac. Pharmacy, Cairo Univ.*, vol. 53, no. 2, pp. 195–205, 2015, doi: 10.1016/j.bfopcu.2015.10.004.
- xvii. N. R. M. R. P. T. B. I. D. R. M. M. R. M. Harshad Rajendra Mene, "Formulation aspects in development of controlled porosity osmotic pump tablet," *Pharm. Biol. Eval.*, vol. 3, no. 3, pp. 1–18, 2016.
- xviii. R. A. Keraliya et al., "Osmotic Drug Delivery System as a Part of Modified Release Dosage Form," *ISRN Pharm.*, vol. 2012, pp. 1–9, 2012, doi: 10.5402/2012/528079.
- xix. K. Derakhshandeh and M. Ghasemnejad Berenji, "Development and optimization of buspirone oral osmotic pump tablet," *Res. Pharm. Sci.*, vol. 9, no. 4, pp. 233–241, 2014.
- xx. H. Roy and G. Pradhan, "Formulation and Evaluation of Osmotically Controlled Delivery of Lamivudine Tablet," *Int. J. Med. Nanotechnol.*, vol. 2, no. 5, pp. 2394–4269, 2015.
- xxi. P. Tran, Y. C. Pyo, D. H. Kim, S. E. Lee, J. K. Kim, and J. S. Park, "Overview of the manufacturing methods of solid dispersion technology for improving the solubility of poorly water-soluble drugs and application to anticancer drugs," *Pharmaceutics*, vol. 11, no. 3, pp. 1–26, 2019, doi: 10.3390/pharmaceutics11030132.
- xxii. N. Li et al., "Preparation and in vitro/in vivo evaluation of azilsartan osmotic pump tablets based on the preformulation investigation," *Drug Dev. Ind. Pharm.*, vol. 45, no. 7, pp. 1079–1088, 2019, doi: 10.1080/03639045.2019.1593441.
- xxiii. M. A. J. Bhange, M. R. S. Bandal, and M. S. D. Shinde, "Formulation And Evaluation Of Osmotically Controlled Drug Delivery System Of An Anti-Diabetic Drug," *J. Adv. Zool.*, vol. 14, no. 7, pp. 535–550, 2024, doi: 10.53555/jaz.v45i2.4599.
- xxiv. M. T. Saleem, M. H. Shoaib, R. I. Yousuf, and F. Siddiqui, "RSM and AI based machine learning for quality by design development of rivaroxaban push-pull osmotic tablets and its PBPK modeling," *Sci. Rep.*, vol. 15, no. 1, pp. 1–22, 2025, doi: 10.1038/s41598-025-91601-z.
- xxv. V. V. Kumar and Y. Ismail, "Formulation and Optimization of Budesonide Colon-Targeted Tablets Using Controlled Porosity Osmotic Pump Technology," *Int. J. Appl. Pharm.*, vol. 17, no. 1, pp. 59–67, 2025, doi: 10.22159/ijap.2025v17i1.52544.
- xxvi. N. H. T. An, H. P. Van, X. D. Thanh, Q. Le Dinh, and D. N. T. Thanh, "Formulation and evaluation of controlled porosity osmotic pump tablets of verapamil hydrochloride," *Minist. Sci. Technol. Vietnam*, vol. 67, no. 2, pp. 100–108, 2025, doi: 10.31276/vjste.2024.0066.
- xxvii. M. R. Reddy, "Formulation and Evaluation of Osmotic Release Tablet of Glipizide," vol. 2024, no. 9, pp. 104–109, 2024.
- xxviii. S. Choudhary, C. Subrahmanyam, and K. Priyanka, "Osmotic Drug Delivery System of Nicorandil: Design and Evaluation," *Int. J. Appl. Pharm.*, vol. 16, no. 3, pp. 119–128, 2024, doi: 10.22159/ijap.2024v16i3.50298.
- xxix. S. Syed, I. Syed, and R. Marathe, "Formulation, development and evaluation of an osmotic drug delivery system for lornoxicam," *Istanbul J. Pharm.*, vol. 53, no. 1, pp. 10–21, 2023, doi: 10.26650/istanbuljpharm.2023.1058131.
- xxx. R. A. Thomas et al., "Journal of Innovations in Applied Pharmaceutical Science [ JIAPS ] COMPARATIVE INSILICO DOCKING STUDY," *J. Innov. Appl. Pharm. Sci.*, vol. 8, no. 3, pp. 39–44, 2023.
- xxxi. S. Ahmad, T. J. Shaikh, J. Patil, A. Meher, D. Chumbhale, and H. Tare, "Osmotic Release Oral Tablet Formulation, Development, and Evaluation of an Anti-epileptic Drug," *Int. J. Drug Deliv. Technol.*, vol. 13, no. 1, pp. 305–312, 2023, doi: 10.25258/ijddt.13.1.50.
- xxxii. Vyshnavi, V. Anjaneyulu, and G. V. Kumar, "Formulation and evaluation of osmotic tablets of Ranolazine," *Int. J. Pharm. Res. Technol.*, vol. 13, no. 2, pp. 1–6, 2023, doi: 10.31838/ijpr/13.02.01.
- xxxiii. Aslam et al., "Fabrication of Stimuli-Responsive Quince/Mucin Co-Poly (Methacrylate) Hydrogel Matrices for the Controlled Delivery of Acyclovir Sodium: Design, Characterization and Toxicity Evaluation," *Pharmaceutics*, vol. 15, no. 2, pp. 1–23, 2023, doi: 10.3390/pharmaceutics15020650.
- xxxiv. K. Chaitanya and S. Velmurugan, "Formulation and evaluation of levodopa effervescent floating tablets," *Int. J. Pharm. Pharm. Sci.*, vol. 7, no. 5, pp. 189–193, 2015.
- xxxv. R. Gundu, S. Pekamwar, S. Shelke, D. Kulkarni, and S. Shep, "Development, optimization and pharmacokinetic evaluation of biphasic extended-release osmotic drug delivery system of tiroprium chloride for promising application in treatment of overactive bladder," *Futur. J. Pharm. Sci.*, vol. 7, no. 1, 2021, doi: 10.1186/s43094-021-00311-6.
- xxxvi. H. P. N. Ahmed Sholapur et al., "Quality by Design Approach for Design, Development and Optimization of Orally Disintegrating Tablets of Montelukast Sodium," *Int. J. Pharm. Investig.*, vol. 11, no. 3, pp. 288–295, 2021, doi: 10.5530/ijpi.2021.3.51.
- xxxvii. S. Nandi, A. Banerjee, and K. H. Reza, "Formulation and evaluation of enteric coated elementary osmotic tablets of aceclofenac," *Turkish J. Pharm. Sci.*, vol. 18, no. 4, pp. 498–509, 2021, doi: 10.4274/tjps.galenos.2020.03443.
- xxxviii. P. Jain and P. S. Naruka, "Formulation and evaluation of fast dissolving tablets of valsartan," *Int. J. Pharm. Pharm. Sci.*, vol. 11, no. 1, pp. 219–226, 2009.
- xxxix. K. Sahoo, N. K. Sahoo, S. R. M. Rao, and M. Sudhakar, "Formulation and Optimization of Controlled Porosity Osmotic Pump Tablets of Lamivudine using Sodium Chloride as Osmogen for the Treatment of AIDS," *Madridge J. Nov. Drug Res.*, vol. 2, no. 1, pp. 94–101, 2018, doi: 10.18689/mjndr-1000114.
- xl. S. Taymouri, A. Mostafavi, and S. Zaretaghiabadi, "Design, Formulation and Evaluation of Physicochemical Properties of Valacyclovir Effervescent Tablet," *Trends Pharm. Sci.*, vol. 8, no. 3, pp. 135–146, 2022, doi: 10.30476/TIPS.2022.95385.1145.
- xli. Khan, H. Sciences, M. M. Kanakal, A. Kalusalingam, H. Sciences, and M. J. Sadik, "Development and in-vivo evaluation of Repaglinide Osmotic Drug Delivery SYSTEM USING," 2023, doi: 10.48047/ecb/2023.12.si10.00147.
- xlii. Y. Almoshari, "Osmotic Pump Drug Delivery Systems—A Comprehensive Review," *Pharmaceutics*, vol. 15, no. 11, 2022, doi: 10.3390/ph15111430.

©2025 The authors

This is an Open Access article

distributed under the terms of the Creative Commons Attribution (CC BY NC), which permits unrestricted use, distribution, and reproduction in any medium, as long as the original authors and source are cited. No permission is required from the authors or the publishers. (<https://creativecommons.org/licenses/by-nc/4.0/>)